Biochimica et Biophysica Acta 892 (1987) 108–117
Elsevier

BBA 42535

Inhibition of yeast mitochondrial F_1-ATPase, F_0F_1-ATPase and submitochondrial particles by rhodamines and ethidium bromide *

Hans-Joachim Wieker, Dietrich Kuschmitz and Benno Hess

Max-Planck-Institut für Ernährungsphysiologie, Dortmund (F.R.G.)

(Received 16 December 1986)

Key words: ATPase inhibition, H^+; Rhodamine 6G; Ethidium bromide; (Yeast mitochondria)

ATP hydrolysis by F_1-ATPase is strongly inhibited by cationic rhodamines; neutral rhodamines are very poor inhibitors. Rhodamine 6G is a noncompetitive inhibitor of purified F_0F_1-ATPase and submitochondrial particles, however, an uncompetitive inhibitor of F_1-ATPase ($K_I \approx 2.4$ μM for all three enzyme forms). Ethidium bromide is a noncompetitive inhibitor of F_0F_1-ATPase, submitochondrial particles and also F_1-ATPase ($K_I \approx 270$ μM). Neither of the inhibitors affects the negative cooperativity ($n_H \approx 0.7$). The non-identical binding sites for rhodamine 6G and ethidium bromide are located on the F_1-moiety and are topologically distinct from the catalytic site. Binding of the inhibitors prevents the conformational changes essential for energy transduction. It is concluded that the inhibitor binding sites are involved in proton translocation. In F_1-ATPase, binding of MgATP at a catalytic site causes conformational changes, which allosterically induce the correct structure of the rhodamine 6G binding site. In F_0F_1-ATPase, this conformation of the F_1-moiety exists a priori, due to allosteric interactions with F_0-subunits. The binding site for ethidium bromide on F_1-ATPase does not require substrate binding at the catalytic site and is not affected by F_0F_1-subunit interactions.

Introduction

Fluorescent voltage-sensitive dyes are valuable tools for measuring transmembrane potentials of cells and organelles, e.g., mitochondria [1–4]. However, it has also been shown that especially the positively charged dyes are potent inhibitors of several mitochondrial energy-transducing activities [4–7]. In some cases, e.g., rhodamine 6G and ethidium bromide, energy-dependent H^+ ejection from mitochondria could be correlated to effects of the dyes on the ATPase/ATP synthase system [5,6]. Thus, it is suggestive that these dyes interact with the proton-conducting pathway of the H^+-ATPase. With respect to specific effects of such dyes on mitochondrial H^+-ATPase, however, contradictory results are reported and the localization of the dye binding site is not clear at all: rhodamine 6G was found to inhibit purified F_0F_1 and submitochondrial particles but not purified F_1 [6]; rhodamine 123 inhibits submitochondrial particles and partially purified F_1 [4]. Both dyes inhibit

* Part of this work was presented at the 4th European Bioenergetics Conference, Prague, August 1986.

Abbreviations: P_i, inorganic phosphate; F_1, the ATPase component of ATP synthase; F_0, the proton-conducting component (membrane sector) of ATP synthase; Hepes, 4-(2-hydroxyethyl)-1-piperazinethanesulfonic acid; Rho6G, rhodamine 6G.

Correspondence: H.-J. Wieker, Max-Planck-Institut für Ernährungsphysiologie, Rheinlanddamm 201, D-4600 Dortmund, F.R.G.

purified F_0F_1, but only in the presence of phospholipid vesicles [8], rhodamine 6G being 70-times more effective than rhodamine 123. Ethidium bromide inhibits ATP synthesis in intact mitochondria, but in submitochondrial particles only after incorporation inside the particles [5]; ATP hydrolysis by submitochondrial particles is strongly inhibited, while F_1 is barely affected [7]; ethidium bromide is a noncompetitive inhibitor of membrane-bound F_0F_1 as well as isolated F_1 [9,10]. Diazidoethidium bromide, however, does not react with F_1, but covalently labels a subunit of the F_0-moiety in mitochondria and soluble F_0F_1 [11].

Concerning mitochondrial H^+-ATPase, this work was performed with the aim to answer the following questions: (i) What is the mechanism of the enzyme inhibitor interactions? (ii) Is there a relationship between the structure of the dyes and the mechanism of inhibition? (iii) Do the inhibitors affect the enzyme substrate interactions, the catalytic process or the proton translocation? (iv) Are the binding sites of structurally different dyes such as rhodamine 6G and ethidium bromide located on the F_0- or on the F_1-sector? Therefore, kinetic studies on the inhibition of ATP hydrolysis by various rhodamines and ethium bromide were performed under identical conditions with three forms of mitochondrial H^+-ATPase from *S. cerevisiae*: purified F_1, purified F_0F_1 and submitochondrial particles.

Materials and Methods

Rhodamine B, 3B, 6G, 19, 110, 116, 123 (laser grade) were purchased from Kodak Chemicals, Rochester; ethidium bromide and Hepes from Sigma, Munich. Pyruvate kinase, lactate dehydrogenase (both in 50% glycerol), ATP, NADH and phospho*enol*pyruvate were bought from Boehringer GmbH, Mannheim. All other chemicals used were p.a. grade and purchased from E. Merck, Darmstadt.

Yeast mitochondrial F_1-ATPase with a specific activity of 160 U/mg at pH 7.0 (about 190 U/mg at pH 8.0) was prepared from *Saccharomyces cerevisiae* by chloroform extraction as described elsewhere [12]. The enzyme was stored as an ammonium sulfate suspension and prior to use diluted with a 1:1 glycerol/water mixture containing 0.25 M sorbitol, 50 mM Tris/HCl, 50 mM NaCl and 2 mM EDTA, adjusted to pH 8.0. To remove the ammonium sulfate, 1 ml was centrifuged through a 5 ml syringe with Sephadex G-25 equilibrated with the same buffer.

With slight modifications described elsewhere [13], yeast mitochondria were prepared according to Guérin et al. [14], submitochondrial particles according to Harmon [15], and F_0F_1 was prepared by the α-lysolecitin extraction method of Penin et al. [16]. Submitochondrial particles and F_0F_1 were stored in 0.25 M sorbitol, 10 mM Tris-HCl (pH 7.5) at −70 °C and prior to use diluted with the glycerol/water mixture as above.

Relative activities were measured spectrophotometrically at 25 °C in an 'optimal assay': the final volume of the cuvette (2.02 ml) was made up of 50 mM Tris/acetic acid, adjusted to pH 8.0 with KOH, 2 mM phospho*enol*pyruvate, 3 mM $MgCl_2$, 2 mM ATP, 0.4 mM NADH, 50 μg/ml pyruvate kinase, 25 μg/ml lactate dehydrogenase and the appropriate concentrations of inhibitors. In case of submitochondrial particles and F_0F_1, 1 mM KCN was added. The reaction was started with 20 μl of the diluted enzyme solutions.

Initial velocities v were determined spectrophotometrically at 25 °C at constant concentrations of inhibitor [I], the substrate concentration [S] being varied from 5 μM to 2.5 mM MgATP. The final volume of the cuvette (2.02 ml) was made up of 0.2 M Hepes, adjusted to pH 7.0 with KOH, 4 mM phospho*enol*pyruvate, 0.5 mM NADH, 50 μg/ml pyruvate kinase, 50 μg/ml lactate dehydrogenase and the appropriate concentrations of $MgCl_2$, ATP and inhibitor. Using a dissociation constant of 0.13 mM at pH 7.0 for the MgATP complex [17,18], the total amounts of Mg^{2+} and ATP were adjusted to yield the desired concentrations of the substrate MgATP and 1.0 mM free Mg^{2+}. In case of submitochondrial particles and F_0F_1, 1 mM KCN was added. The reaction was started with 20 μl of the enzyme solutions. In a second series of experiments, v was determined at constant [S] and variable [I]. Separate measurements ensured, that the inhibitors had no effect on the coupled assay system.

Evaluation of kinetic parameters

When initial velocities v were measured as a function of substrate concentration [S] at constant concentrations of inhibitor [I], the data (20–25 per curve) were analyzed according to the Hill equation

$$v = \frac{V_{max}}{1+\left(\frac{[S]_{0.5}}{[S]}\right)^{n_H}} \quad (1)$$

using the method of Wieker et al. [19], which evaluates the maximal velocity V_{max}, the interaction coefficient n_H and the substrate concentration $[S]_{0.5}$, giving $\frac{1}{2}V_{max}$ by an iteration procedure. When v was measured as function of [I] at constant [S], fractional inhibitions η were calculated

$$\eta = 1 - \frac{v}{v_0} \quad (2)$$

where v_0 is the velocity in the absence of inhibitor. These data (15–20 per curve) were analyzed according to

$$\eta = \frac{\eta_{max}}{1+\left(\frac{[I]_{0.5}}{[I]}\right)^{n_H}} \quad (3)$$

and n_H, the maximal inhibition η_{max} and the inhibitor concentration $[I]_{0.5}$, giving $\frac{1}{2}\eta_{max}$ were determined by the same procedure [19].

Regardless of the chemical mechanism involved in the reaction, there are three types of inhibition classifying an inhibitor.

(1) Noncompetitive inhibition (Scheme I) is characterized by the existence of both an enzyme-inhibitor complex EI and an enzyme-substrate-inhibitor complex ESI.

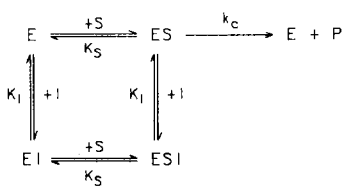

Scheme I

k_c, K_S and K_I denote the velocity constant of the rate-limiting step, the substrate dissociation constant and the inhibitor constant, respectively. Scheme I predicts that $[S]_{0.5}$ is independent of [I]

$$[S]_{0.5} = K_S \quad (4)$$

while $1/V_{max}$ is a linear function of [I]

$$\frac{1}{V_{max}} = \frac{1}{k_c}\left(1+\frac{[I]}{K_I}\right) \quad (5)$$

and $[I]_{0.5}$ is independent of [S]

$$[I]_{0.5} = K_I \quad (6)$$

(2) Uncompetitive inhibition (Scheme II) is characterized by the existence of only ESI, but not EI.

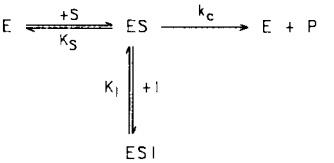

Scheme II

Scheme II predicts that both $1/[S]_{0.5}$

$$\frac{1}{[S]_{0.5}} = \frac{1}{K_S}\left(1+\frac{[I]}{K_I}\right) \quad (7)$$

and $1/V_{max}$ (Eqn. 5) are linear functions of [I], and that $[I]_{0.5}$ depends linearly on $1/[S]$

$$[I]_{0.5} = K_I\left(1+\frac{K_S}{[S]}\right) \quad (8)$$

It is a characteristic feature of uncompetitive (also called anticompetitive) inhibition that the apparent affinities of substrate and inhibitor are mutually increased.

(3) Competitive inhibition is characterized by the existence of only EI, but not ESI, and predicts linear functions of $[S]_{0.5}$ of [I] and $[I]_{0.5}$ of [S], while V_{max} is independent of [I]. As will be seen in the results, all inhibitors investigated strongly affect V_{max}. Therefore, competitive inhibition needs not to be considered.

The type of inhibition was determined by replotting V_{max}, $[S]_{0.5}$ and $[I]_{0.5}$ according to Eqns 4–8, and the kinetic parameters k_c, K_S and K_I are obtained from these replots by least-squares fitting. In addition, replots of n_H were used to

establish whether the inhibitors affect to negative cooperativity of MgATP or whether the binding of the inhibitors is cooperative.

The negative cooperativity, found with H^+ATPases from yeast mitochondria and other sources (Ref. 18 and references therein), may rise the question whether Schemes I and II can really be applied. However, as demonstrated for yeast mitochondrial F_1 [18], this procedure is valid to characterize the type and to quantify the strength of inhibition. The real problem then will be to identify the individual reaction steps governed by k_c, K_S and K_I.

Results

The inhibition of F_1 by different rhodamines (I), the substituents of which are given in Table I, and of ethidium bromide (II) were investigated in the 'optimal assay'. Due to the poor solubility of some rhodamines in water, all dyes were dissolved in ethanol and the inhibition η_{50} obtained with [I] = 50 μM was measured (Table I).

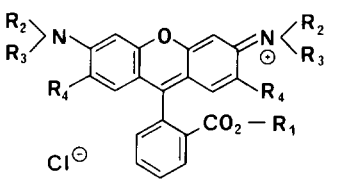

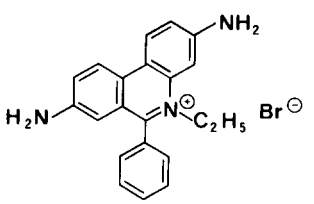

Structures I (above) and II (below).

All rhodamines with a free carboxyl group (R_1 = H), which are neutral at physiological pH, i.e., rhodamine B, 19, 110, 116, are weak inhibitors with $\eta_{50} \leq 0.1$. Rhodamines with an ester group ($R_1 = C_2H_5$), which are positively charged, i.e., rhodamine 6G, 3B, are strong inhibitors with $\eta_{50} \geq 0.9$. Neither a substituent R_4 at the heterocycle nor a second substituent R_3 at the amino group is essential for the inhibition; however, one substituent R_2 at the amino group seems to be necessary, since rhodamine 123 is significantly less inhibitory than rhodamine 6G and 3B. Although positively charged, ethidium bromide is a weak inhibitor with $\eta_{50} = 0.17$ (Table I). This may be due to either the lack of any substituent at the amino groups, or to the different structures of the heterocycles, or to non-identical binding sites for rhodamines and ethidium bromide or to different mechanisms of inhibition.

TABLE I

STRUCTURE AND FUNCTION OF RHODAMINES

R_1–R_4 are the substituents in structure I, η_{50} is the inhibition of F_1-ATPase measured with [I] = 50 μM. At physiological pH the rhodamines with R_1 = H are neutral, those with $R_1 \neq$ H are positively charged.

	R_1	R_2	R_3	R_4	η_{50}
Rho 6G	C_2H_5	C_2H_5	H	CH_3	0.90
Rho 3B	C_2H_5	C_2H_5	C_2H_5	H	0.90
Rho 123	CH_3	H	H	H	0.25
Rho 19	H	C_2H_5	H	CH_3	0.09
Rho B	H	C_2H_5	C_2H_5	H	0.06
Rho 110	H	H	H	H	0.0
Rho 116	H	CH_3	H	H	0.08
Ethidium bromide (structure II)					0.17

To compare the inhibitory effects of rhodamine 6G on F_1, F_0F_1 and submitochondrial particles, relative activities were measured in the 'optimal assay' (the high solubility of rhodamine 6G enables the use of aqueous solutions). As shown in Fig. 1, the inhibition of the three enzyme forms by rhodamine 6G is obviously identical. Since these measurements were performed at saturating substrate concentration, the curves in Fig. 1 point to an effect of rhodamine 6G on V_{max}, and therefore noncompetitive or uncompetitive inhibition is expected. In general, a decrease of V_{max} can also result from covalent binding of an inhibitor. Dilution experiments (not shown), however, proved full reversibility of all inhibitions reported here.

Initial velocity measurements with F_1 as functions of [MgATP] at constant [Rho6G], and data analysis according to Eqn. 1 show that both V_{max} and $[S]_{0.5}$ decreased with [Rho6G], while n_H (with a mean value of $n_H = 0.76$) was independent of [I].

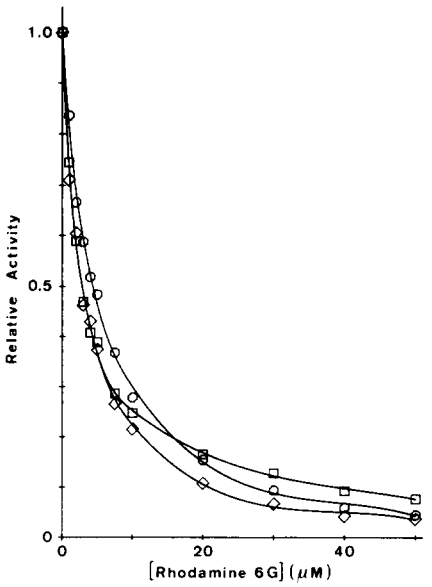

Fig. 1. Relative activity v/v_0 as a function of [rhodamine 6G]. The measurements were performed with F_1-ATPase (□), F_0F_1-ATPase (○) and submitochondrial particles (◇) in the 'optimal assay'. The curves are spline approximations using subroutine VB05B of the Harwell subroutine library.

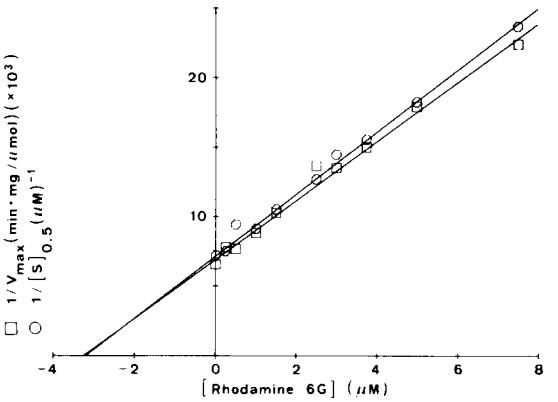

Fig. 2. Linear least-squares fits of $1/V_{max}$ and $1/[S]_{0.5}$ as functions of [rhodamine 6G] (Eqns. 5 and 7). V_{max} and $[S]_{0.5}$ were determined from v vs. [s] (Eqn. 1) measured with F_1-ATPase.

Replots of $1/V_{max}$ and $1/[S]_{0.5}$ as functions of [I] according to Eqns 5 and 7 (Fig. 2) revealed the following kinetic constants (see Scheme II and Table II): $k_c = 145.2$ μmol/min per mg, $K_S = 140.3$ μM and $K_I = 3.2$ μM. The linear dependence between $1/[S]_{0.5}$ and [I] corresponding to Eqn. 7 characterizes rhodamine 6G as an uncompetitive inhibitor of F_1, which can only bind to the F_1-MgATP complex (Scheme II). From the independence of n_H it follows that the binding of rhodamine 6G is non-cooperative and does not affect the negative cooperativity of MgATP.

Also with F_1, fractional inhibitions η (Eqn. 2) were measured as functions of [Rho6G] at constant [MgATP] and analyzed according to Eqn. 3. The replot of $[I]_{0.5}$ vs. $1/[S]$ according to Eqn. 8 (Fig. 3) confirms that rhodamine 6G is an uncompetitive inhibitor of F_1. The resulting parameters $K_S = 119.8$ μM and $K_I = 2.0$ μM (Table II) are in good agreement with the values above. η_{max} shows only a slight dependence on [S] (Fig. 4), and the

TABLE II

KINETIC PARAMETERS OF F_1-ATPase, F_0F_1-ATPase AND SUBMITOCHONDRIAL PARTICLES

The parameters (±S.D.) are obtained from replots (Eqns. 5, 7 and 8) by least-squares fits or are averages (Eqn. 4). The n_H obtained from v vs. [S] are mean values. The three parameter sets for F_1-ATPase are obtained with different enzyme preparations.

	n_H	k_c (U/mg)	K_S (μM)	K_I (μM)	
				Rho6G	ethidium bromide
F_1-ATPase	0.76±0.04	145.2±3.4	140.3± 2.8	3.23±0.09	
F_1-ATPase			119.8± 2.1	1.97±0.02	
F_1-ATPase	0.66±0.03	135.2±3.5	109.4±11.0		279.1±10.0
F_0F_1-ATPase	0.82±0.02	14.8±1.3	76.8± 6.3	1.95±0.20	256.0± 9.5
submitochondrial particles	0.76±0.03	4.9±0.2	78.9± 3.2	1.91±0.20	263.6± 8.0

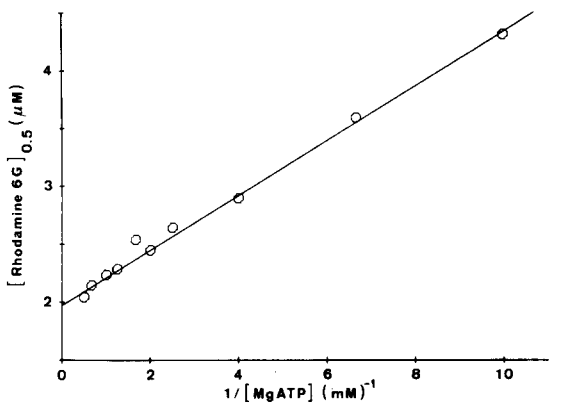

Fig. 3. Linear least-squares fit of [rhodamine 6G]$_{0.5}$ as a function of 1/[MgATP] (Eqn. 8). The [I]$_{0.5}$ were determined from η vs. [I] (Eqn. 3) measured with F_1-ATPase.

average value of $\eta_{max} = 0.93$ means total inhibition of F_1 by rhodamine 6G, i.e., the ESI complex (Scheme II) cannot perform the rate-limiting step. The interaction coefficient n_H (Fig. 4) increases from $n_H = 0.77$ at [MgATP] ≤ 0.25 mM to $n_H = 0.95$ at [MgATP] ≥ 1.0 mM. This dependence is also consistent with uncompetitive inhibition (Scheme II): at low [S], i.e., [ES] $\ll$ [E], the degree of saturation with substrate ([ES] + [ESI]) increases with [I], and η vs. [I] reflects the cooperativity of additional substrate binding to the enzyme. At high [S], i.e., [ES] $\gg$ [E], no cooperativity of substrate binding is observable, and therefore η vs. [I] should be governed by $n_H \approx 1$, if binding of the inhibitor to [ES] is non-cooperative itself.

A quite different behaviour was found with F_0F_1, both purified and in submitochondrial particles: $[S]_{0.5}$ is independent of [Rho 6G], as demonstrated for F_0F_1 in Fig. 5 (for better comparison with Fig. 2, $1/[S]_{0.5}$ is plotted). The mean value of $[S]_{0.5}$ yielded $K_S = 76.8$ μM (parameters for submitochondrial particles are listed in Table II). This independence of $[S]_{0.5}$ from [I] shows that Eqn. 4 is valid and not Eqn. 7 and that binding of I to E and ES (Scheme I) is not affected by MgATP. Thus, rhodamine 6G is characterized as a non-competitive inhibitor of F_0F_1 and submitochondrial particles. As in case of F_1, V_{max} decreased with [Rho6G], and the replot of $1/V_{max}$ vs. [I] in Fig. 5 yielded $k_c = 14.8$ μmol/min per mg and $K_I = 2.0$ μM (Table II), in good agreement with the K_I of F_1. The interaction coefficient is also independent of [I] (mean value of n_H, 0.82), showing that binding of rhodamine 6G to F_0F_1 is non-cooperative and does not affect the negative cooperativity of MgATP. It should be noted that a characteristic property of the yeast mitochondrial enzyme can be deduced from Table II: ratios F_1/ F_0F_1/ submitochondrial particles of about 10 : 1 : 0.3 for k_c and of about 2 : 1 : 1 for K_S are generally measured.

Initial velocity measurements were also performed with the structurally quite different ethidium bromide (see Structure II above). With

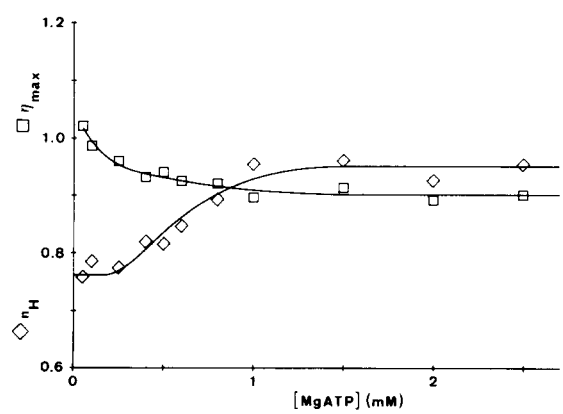

Fig. 4. Replots of η_{max} and n_H as functions of [MgATP]. η_{max} and n_H were determined from η vs. [I] (equation 3) with F_1-ATPase.

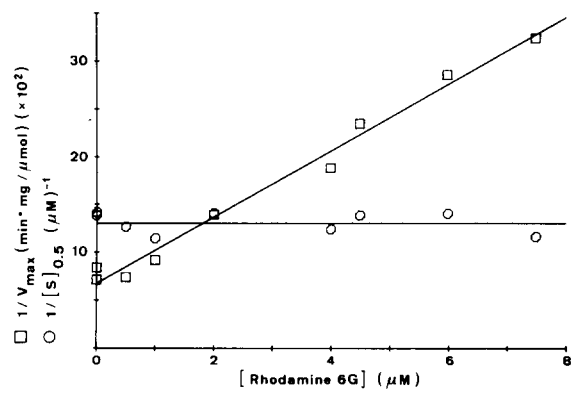

Fig. 5. Linear least-squares fit of $1/V_{max}$ as a function of [rhodamine 6G] (Eqn. 5). The horizontal line corresponds to the mean value of the $[S]_{0.5}$ (Eqn. 4). V_{max} and $[S]_{0.5}$ were obtained from v vs. [S] (Eqn. 1) measured with F_0F_1-ATPase.

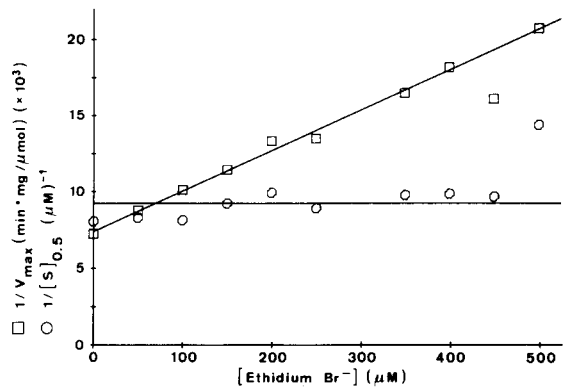

Fig. 6. Linear least-squares fit of $1/V_{max}$ as a function of [ethidium bromide] (Eqn. 5). The horizontal line corresponds to the mean value of the $[S]_{0.5}$ (Eqn. 4). V_{max} and $[S]_{0.5}$ were obtained from v vs. [S] (Eqn. 1) measured with F_1-ATPase.

F_1 as well as with F_0F_1 and submitochondrial particles this inhibitor only decreased V_{max}, while $[S]_{0.5}$ and n_H were independent of the ethidium bromide concentration. The replot of $1/V_{max}$ vs. [I] in Fig. 6 revealed $k_c = 135.2$ μmol/min per mg and $K_I = 279.1$ μM for F_1, and the mean value of $[S]_{0.5}$ (Fig. 6) yielded $K_S = 109.4$ μM (the parameters for F_0F_1 and submitochondrial particles are given in Table II). The independence of $[S]_{0.5}$ from [I], which is only consistent with Eqn. 4, shows that binding of I to E and ES (Scheme I) is not affected by MgATP, and classifies ethidium bromide as a noncompetitive inhibitor of F_1 as well as F_0F_1 and submitochondrial particles. The independence of n_H from [I] (mean value of n_H with F_1, 0.66) shows that binding of ethidium bromide to all three enzyme forms is non-cooperative and does not affect the negative cooperativity of MgATP, as in the case of rhodamine 6G. In comparison, ethidium bromide is 130-times less effective than rhodamine 6G (see K_I in Table II); however, the most striking difference is the noncompetitive inhibition of F_1 by ethidium bromide and the uncompetitive inhibition of F_1 by rhodamine 6G.

Discussion

Yeast mitochondrial ATPase is a complex enzyme which exerts the characteristic negative cooperativity of ATP hydrolysis like other comparable ATPase/ATP synthases. Therefore, Schemes I and II cannot be regarded as schematic presentations of the ATPase reaction, but they are nevertheless sufficient to characterize the type of inhibition and to deduce the enzyme-ligand complexes in the reaction mechanism. All conclusions derived then have to be interpreted on the basis of special mechanisms developed for these H^+-ATPases. In the following discussion, the binding-change mechanism [20–23], assuming three equivalent catalytic sites modulated by non-equivalent interactions during the catalytic process, shall serve for a mechanistic interpretation. However, a discussion based on models with distinct catalytic (two or three) and regulatory sites [24,25] will lead to the same conclusions.

Regardless of any mechanism, the results demonstrate that the binding sites for rhodamine 6G and ethidium bromide are located on the F_1-sector of the enzymes, since F_1, F_0F_1 and submitochondrial particles are inhibited by these dyes with the same K_I values (Table II) for rhodamine 6G and for ethidium bromide. Furthermore, it can be concluded that both inhibitors bind to negatively charged residues on the enzymes, because only positively charged rhodamines are effective inhibitors (Table I) and ethidium bromide is also positively charged.

The noncompetitive inhibition of F_0F_1 and submitochondrial particles by rhodamine 6G predicts that both an EI and an ESI complex (Scheme I) are formed in the reaction course. It follows from the independence of $[S]_{0.5}$ from [I] (Fig. 5), that substrate and inhibitor bind independently at topologically different sites of the enzyme, and that rhodamine 6G has the same affinity for free F_0F_1 as for the F_0F_1-MgATP complex. The linear dependence of $1/V_{max}$ on [I] (Fig. 5) proves, that the ESI complex cannot perform the rate-limiting step. The uncompetitive inhibition of isolated F_1 by rhodamine 6G predicts that only the ESI complex is formed and that the inhibitor cannot bind to the free enzyme (Scheme II). Consequently, binding of MgATP to F_1 is accompanied by a conformational change which induces the correct structure of the rhodamine 6G binding site. Binding of the inhibitor to the F_1-MgATP complex prevents allosterically the rate-limiting step, as with F_0F_1.

Ethidium bromide is a noncompetitive inhibi-

tor of all three enzyme forms investigated with identical affinities for the free enzymes and for the ES complexes (Fig. 6, Table II). As outlined above, it follows from the type of inhibition (Scheme I), that the binding site of this inhibitor is topologically different from the catalytic site and that ethidium bromide allosterically blocks the rate-limiting step. The striking difference to rhodamine 6G, however, is that ethidium bromide binds to free F_1 without previous induction of its binding site by MgATP. Furthermore, the K_I is about 130-times higher. Therefore, the binding site of ethidium bromide, always available in F_1, and the binding site of rhodamine 6G, not available in free F_1, cannot be identical.

Recently, it was demonstrated that product dissociation is the rate-limiting step, while the interconversion of $ATP + H_2O$ into $ADP + P_i + H^+$ occurs with negligible change in free energy [21], i.e., the energy difference between substrates and products has to be stored in the protein structure. This energy is dissipated by proton transfer processes, accompanied by changes in the ligand affinity and subunit interactions [20,22]. In case of inhibition of F_0F_1 by rhodamine 6G, however, it seems to be rather unreliable that the inhibitor prevents the dissociation of ADP and/or P_i, while it has no effect on the binding of ATP (in ATP synthesis, the dissociation of ATP is the rate-limiting step [21]). However, the third product of ATP hydrolysis must also be considered: the proton generated at the catalytic site of F_0F_1 is transferred through F_1 towards F_0, where it is released into the medium, as shown by proton pumping of F_0F_1 in vesicles. The finding that only positively charged rhodamines are potent inhibitors (Table I) suggests that rhodamine 6G binds to negatively charged proton binding groups of the F_1-sector. These residues cannot be involved in the proton-generating process, because they are not part of the catalytic site as outlined above. Therefore, these groups are either directly involved in the proton-transfer reaction or take part in conformational changes essential for proton translocation. Regardless of a direct or indirect participation of the rhodamine 6G binding site in the proton transfer and regardless of any H^+/ATP stoichiometry, binding of rhodamine 6G, as demanded by the kinetic analysis, allosterically blocks the rate-limiting proton transfer.

According to the binding change mechanism [20,23], the negative cooperativity of ATP hydrolysis results from alterations of the substrate affinity, due to proton translocation, and from a rate enhancement of product dissociation, caused by substrate binding at another catalytic site. Binding of rhodamine 6G blocks these processes, but since all enzyme species with bound inhibitor do not contribute to the reaction velocity, the shape of the v vs. [S] curves is determined by those enzyme species only, which are not occupied by the inhibitor. Consequently, it is expected that the inhibitor does not affect the homotropic negative cooperativity. In fact, in all cases n_H remains constant (Table II), and the binding of the inhibitor itself is non-cooperative.

The uncompetitive inhibition of F_1 by rhodamine 6G predicts, that binding of MgATP at the catalytic site induces a conformational change, resulting in the correct structure of the inhibitor binding site. Recently, conformational changes associated with ATP binding were postulated from lag-phases observed in pre-steady state kinetics [24,25]. These lag-phases were interpreted to result from an activation of F_1 by binding of ATP at an additional regulatory site, however, they can as well be explained by the binding change hypothesis without the assumption of regulatory sites [22,23]. Here the conformational change is derived from the analysis of kinetic data, independent of any mechanistic interpretation. Furthermore, this process occurs in the steady-state of the reaction and therefore cannot be assigned to a slow transition from inactive to active F_1, as suggested in Ref. 25. These conformational states of F_1 and F_0F_1 are schematically depicted in Fig. 7 (additional conformational changes during and after the catalytic step are omitted). With respect to its functional properties, the inhibitor binding site induced in F_1 is obviously identical with that a priori existing in F_0F_1 (Fig. 7), since the K_I-values are identical (Table II). This implies that an analogous conformational change of the F_1-moiety results from interactions between F_0- and F_1-subunits. With the binding site of rhodamine 6G being involved in proton translocation, it follows that the subunit interactions between F_0 and F_1 ensure the transfer of protons from the catalytic

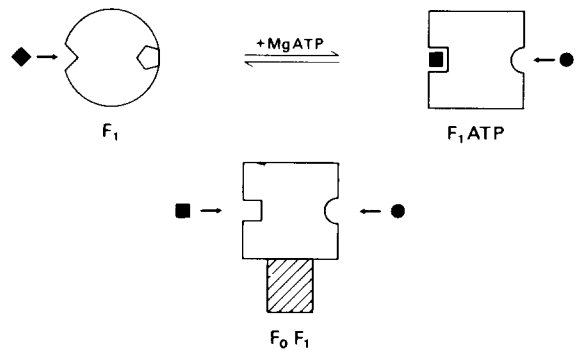

Fig. 7. Schematic representation of the conformational changes occurring in F_1-ATPase and F_0F_1-ATPase. In F_1-ATPase, only the binding site for MgATP (■) is available, and substrate binding is essential to induce the correct structure of the binding site for rhodamine 6G (●). In F_0F_1-ATPase, conformational changes caused by subunit interactions result in the correct binding site for rhodamine 6G, and substrate binding is not essential.

site through F_1- towards F_0-subunits. Thus, in F_0F_1 the F_0-sector is not only a proton channel, but it also regulates the function of the F_1-sector. In isolated F_1, too, the proton generated at the catalytic site is transferred to another site before it is released.

In case of H^+-ATPase from rat liver mitochondria it was concluded, that rhodamine 6G is bound to the F_0-sector, because F_0F_1 and submitochondrial particles were inhibited but not isolated F_1 [6]. In view of our results, however, another interpretation may be, that the rhodamine 6G binding site on the F_1-sector exists on F_0F_1, but cannot be induced by MgATP on isolated liver F_1. Indeed, differences in the primary structure (e.g. Ref. 26) and the regulatory properties (e.g., Ref. 18) are observed with F_1 from different sources.

In summary, the questions asked in the Introduction can now be answered: the structural differences between the two dyes are reflected by quite different affinities and by the uncompetitive inhibition of F_1 by rhodamine 6G and the noncompetitive inhibition of F_1 by ethidium bromide. Both dyes do not affect the enzyme substrate interactions nor the catalytic process of ATP hydrolysis, but allosterically block the proton translocation coupled to ATP hydrolysis. The nonidentical binding sites are both located on the F_1-sector and are topologically different from the catalytic site. Regarding the strength of inhibition (K_I is about 50 times smaller than K_S) and the different mechanisms with F_1 and F_0F_1, rhodamine 6G promises to be a good tool for further investigations concerning subunit interactions, proton translocation and the amino acid residues involved, conformational changes and allosteric effects resulting from substrate binding, as well as interactions between the catalytic sites of yeast mitochondrial H^+-ATPase.

Acknowledgements

The authors thank Mrs. U. Nicolaus and Mr. K.H. Wüster for the preparation of the enzyme, Mrs. Ch. Kebbedies for the skillful performance of the kinetic measurements and Mrs. B. Plettenberg for typing the manuscript.

References

1 Gitler, C., Rubalcava, B. and Caswell, A. (1969) Biochim. Biophys. Acta 193, 479–481
2 Yaginuma, N., Hirose, S. and Inada, Y. (1973) J. Biochem. 74, 811–815
3 Hess, B., Boiteux, A. and Kuschmitz, D. (1983) in Biological Oxidations (Sund, H. and Ullrich, V., eds.), pp. 249–266, Springer-Verlag, Berlin
4 Emaus, R.K., Grunwald, R. and Lemasters, J.J. (1986) Biochim. Biophys. Acta 850, 436–448
5 Higuti, T., Yokota, M., Arakaki, N., Hattori, A. and Tani, I. (1978) Biochim. Biophys. Acta 503, 211–222
6 Higuti, T., Nimi, S., Saito, R., Nakasima, S., Ohe, T., Tani, I. and Yoshimura, T. (1980) Biochim. Biophys. Acta 593, 463–467
7 Peña, A., Chávez, E., Cárabez, A. and Tuena de Gómez-Puyou, M. (1977) Arch. Biochem. Biophys. 180, 522–529
8 Mai, M.S. and Allison, W.S. (1983) Arch. Biochem. Biophys. 221, 467–476
9 Crosby, B., Boutry, M. and Goffeau, A. (1979) Biochem. Biophys. Res. Commun. 88, 448–455
10 Cataldi de Flombaum, M.A. and Stoppani, A.O.M. (1986) Biochem. Intern. 12, 513–519
11 Bastos, R. de N. (1975) J. Biol. Chem. 250, 7739–7746
12 Takeshige, K., Hess, B., Böhm, M. and Zimmermann-Telchow, H. (1976) Hoppe-Seyler's Z. Physiol. Chem. 357, 1605–1622
13 Gómez Maqueo de Covarrubias, M.Y. (1984) Thesis, Ruhr-Universität Bochum
14 Guérin, B., Labbe, P. and Somlo, M. (1979) Methods Enzymol. 55, 149–159
15 Harmon, H.J. (1982) J. Bioenerg. Biomembrane 14, 377–386

16 Penin, F., Godinot, C., Comte, J. and Gautheron, D.C. (1982) Biochim. Biophys. Acta 679, 198–209
17 Markus, M., Plesser, Th., Boiteux, A., Hess, B. and Malcovati, M. (1980) Biochem. J. 189, 421–433
18 Wieker, H.-J. and Hess, B. (1985) Biochim. Biophys. Acta 806, 35–41
19 Wieker, H.-J., Johannes, K.-J. and Hess, B. (1970) FEBS Lett. 8, 178–185
20 Gresser, M.J, Myers, J.A. and Boyer, P.D. (1982) J. Biol. Chem. 257, 12030–12038
21 Grubmeyer, Ch., Cross, R.L. and Penefsky, H.S. (1982) J. Biol. Chem. 257, 12092–12100
22 Cross, R.L., Grubmeyer, Ch. and Penefsky, H.S. (1982) J. Biol. Chem. 257, 12101–12105
23 Boyer, P.D., Kohlbrenner, W.E., McIntosh, D.B., Smith, L.T. and O'Neal, C.C. (1982) Ann. NY Acad. Sci. 402, 65–83
24 Recktenwald, D. and Hess, B. (1977) FEBS Lett. 80, 187–189
25 Roveri, O.A., Muller, J.L.M., Wilms, J. and Slater, E.C. (1980) Biochim. Biophys. Acta 589, 241–255
26 Gregory, R. and Hess, B. (1981) FEBS Lett. 129, 210–214